applied optics

Birefringence images of polycrystalline films of human urine in early diagnostics of kidney pathology

A. V. Dubolazov,[1] N. V. Pashkovskaya,[2] Yu. A. Ushenko,[3,*] Yu. F. Marchuk,[2] V. A. Ushenko,[3] and O. Yu. Novakovskaya[4]

[1]Optics and Publishing Department, Chernivtsi National University, 2 Kotsiubynskyi St., Chernivtsi, Ukraine
[2]Department of Clinical Immunology, Allergology and Endocrinology of Bukovynian State Medical University, 2 Theatral Sq., Chernivtsi, Ukraine
[3]Correlation Optics Department, Chernivtsi National University, 2 Kotsiubynskyi St., Chernivtsi, Ukraine
[4]The Department of Medical Physics and Biological Informatics, Bukovinian State Medical University, 2 Theatral Sq., Chernivtsi, Ukraine
*Corresponding author: yuriyu@gmail.com

Received 2 November 2015; revised 9 January 2016; accepted 9 January 2016; posted 11 January 2016 (Doc. ID 253121); published 24 February 2016

We propose an optical model of the Mueller-matrix description of mechanisms of optical anisotropy of polycrystalline films of urine, namely, optical activity and birefringence. The algorithm of reconstruction of distributions of parameters—optical rotation angles and phase shifts of the indicated anisotropy types—are elaborated upon. The objective criteria of differentiation of urine films taken from healthy donors and albuminuria patients by means of statistical analysis of such distributions are determined. The operational characteristics (sensitivity, specificity, and accuracy) of the Mueller-matrix reconstruction method of the optical anisotropy parameters are defined.

OCIS codes: (260.5430) Polarization; (070.0070) Fourier optics and signal processing; (170.0110) Imaging systems; (170.3880) Medical and biological imaging.

http://dx.doi.org/10.1364/AO.55.000B85

1. INTRODUCTION

The structure of biological tissues can be considered as structurally inhomogeneous. In order to describe the transformation of polarized light by such complex media, it is necessary to involve the most general approaches based on Mueller-matrix formalism. There are many practical techniques based on measurement and analysis of Mueller matrices of investigated biological objects used in biological and medical research [1–9]. Laser polarimetry was formed recently as a new separate approach within matrix optics [10]. One of the main results obtained within the laser polarimetry approach was established as an interconnection between the set of statistical moments of the first–fourth orders characterizing Mueller-matrix elements and parameters of linear birefringence of human biological tissues fibrillar protein networks. This caused the possibility of diagnostics of oncological changes of skin derma, epithelial and connective tissue of human organs, etc. [11–13]. Nevertheless, the technique of laser polarimetry requires further development.

First, some Mueller-matrix elements appear to be unsuitable for biological sample characterization. The reason for this is the azimuthal dependence of the majority of matrix elements (generally 12 of 16 elements changing its values during the sample rotation around the probing axis).

The second reason for the development of laser polarimetry techniques is the fact that mechanisms of optical anisotropy of biological layers are not limited by linear birefringence. The consideration of the impact of other mechanisms, namely, circular birefringence, is topical in the tasks of increasing the range of diagnostic techniques [14–19].

The third reason is the presence of a variety of optically anisotropic biological objects, for which laser polarimetry techniques are not used widely. Such objects include blood and its plasma, urine, bile, saliva, and others biological fluids. The objects of this class are easily accessible and do not require the traumatic surgery of biopsy.

The possibility of polarization investigation of urine for early detection of albuminuria is considered in this research. It is an urgent task of diagnosis of various pathological conditions of human kidneys. Currently, the traditional differential diagnosis of such conditions includes the following steps: analysis of the patient's complaints, biochemical analysis of urine protein, renal ultrasound diagnostics, and professional judgment. The final step or gold standard is the nephrobiopsy of kidney tissue [20–25]. This set of techniques confidently diagnose disease, which corresponds to a moderate (3–30 μg/μmol) and pronounced increase (>30 μg/μmol) in the content of protein

in the urine of the patient [26–28]. Along with this, the unsolved task is the creation of objective, low-cost, and express screening method of albuminuria diagnostics at early stages (<3 μg/μmol) of kidney pathology close to the gold standard.

This research is aimed on generalization of optical anisotropy of optically thin layers of urine films and the development of the method of "azimuthally stable" Mueller-matrix reconstruction of anisotropy parameters of polycrystalline networks in the task of albuminuria diagnostics.

2. BRIEF THEORETICAL BACKGROUND

In this research, we have utilized the model description of phase anisotropy (optical activity and linear birefringence) of the polycrystalline structure of films of biological fluids developed in [11,14–19,29–34]. For simplification of the experimental data understanding in this part of the research, we present basic states of the theory of phase anisotropy of such polycrystalline films.

It has been defined that the experimentally measured matrices possess the following symmetry:

$$\{M\} = \{\mathrm{K}\}\{P\} = m_{11}^{-1} \times \begin{Vmatrix} 1 & 0 & 0 & 0 \\ 0 & m_{22} & m_{23} & m_{24} \\ 0 & m_{32} & m_{33} & m_{34} \\ 0 & m_{42} & m_{43} & m_{44} \end{Vmatrix}. \quad (1)$$

Here, $\{K\}$ is the Mueller matrix of circular birefringence of molecules of amino acids of the following form:

$$\{\mathrm{K}\} = \begin{Vmatrix} 1 & 0 & 0 & 0 \\ 0 & \psi_{22} & \psi_{23} & 0 \\ 0 & \psi_{32} & \psi_{33} & 0 \\ 0 & 0 & 0 & 1 \end{Vmatrix},$$

$$\psi_{ik} = \begin{cases} \psi_{22} = \psi_{33} = \cos 2\theta, \\ \psi_{23} = -\psi_{32} = \sin 2\theta, \end{cases} \quad (2)$$

where ω is the rotation angle of the polarization plane of the light beam.

Linear birefringence of the amino acid chains can be described by the following Mueller matrix $\{P\}$:

$$\{P\} = \begin{Vmatrix} 1 & 0 & 0 & 0 \\ 0 & p_{22} & p_{23} & p_{24} \\ 0 & p_{32} & p_{33} & p_{34} \\ 0 & p_{42} & p_{43} & p_{44} \end{Vmatrix},$$

$$p_{ik} = \begin{cases} p_{22} = \cos^2 2\rho + \sin^2 2\rho \cos\delta; \\ p_{23} = d_{32} = \cos 2\rho \sin 2\rho(1 - \cos\delta); \\ p_{33} = \sin^2 2\rho + \cos^2 2\rho \cos\delta; \\ p_{42} = -p_{24} = \sin 2\rho \sin\delta; \\ p_{34} = -p_{43} = \cos 2\rho \sin\delta; \\ p_{44} = \cos\delta. \end{cases} \quad (3)$$

Here, ρ is the optical axis direction, $\delta = \frac{2\pi}{\lambda}\Delta n l$ is the phase shift between orthogonal components of light beam amplitude, λ is the wavelength, Δn is the birefringence value, and l is the geometrical thickness of the sample.

Analysis of the obtained data [29–34] was performed within the direct task—statistical processing of distribution of experimentally measured matrix elements $M_{ik}(\theta, \rho, \delta)$ with further differentiation of the samples of urine taken from healthy and albuminuria patients. The inverse task of polarization reconstruction of parameters of phase anisotropy was not considered.

To analyze Mueller matrix Eq. (1), we used the model of an optically anisotropic medium, in which two basic types of phase anisotropy exist [10]. According to this model, the process of transformation of laser radiation polarization by urine can be represented in the form of a sequence of the following mechanisms: "optical activity" and "linear birefringence" of the molecules of amino acids and their complexes.

For analytical and practical applications of Eq. (1), we used the data of investigations [1,9]. Here it is shown that the following elements of matrix $\{M\}$ as well as their combinations are azimuthally stable and independent of the sample rotation angle (Ω):

$$\begin{cases} m_{11}(\Omega) = \text{const}, \\ m_{44}(\Omega) = \text{const}, \end{cases} \quad \begin{cases} [m_{22} + f_{33}](\Omega) \equiv \Sigma m_{22;33}(\Omega) = \text{const}, \\ [m_{23} - f_{32}](\Omega) \equiv \Delta m_{23;32}(\Omega) = \text{const}. \end{cases} \quad (4)$$

From Eqs. (1)–(4) we obtain the following azimuthally invariant algorithms of polarization reconstruction of parameters characterizing the phase anisotropy of polycrystalline film of urine:

$$\begin{cases} \delta = \arccos m_{44}, \\ \theta = 0.5 \arctan \frac{\Delta m_{23;32}}{\sum m_{22;33}}. \end{cases} \quad (5)$$

3. ANALYSIS AND DISCUSSION OF EXPERIMENTAL DATA

The experimental part of the research consisted of the following tasks:

A. Determination of Statistically Valid Representative Sampling of Patients with the Known (Referent) Diagnosis

By means of the software product Statmate for 95% confidence interval ($p < 0.05$), a reliable quantity of people in group 1 (donors) and group 2 (albuminuria of <3 μg/μmol) was determined, with $n = 57$.

B. Samples Preparation

We used optically thin films of urine (attenuation factor $\tau < 0.1$), which were formed under identical conditions by placing a drop of urine on optically homogeneous glass. The geometrical thickness of the samples was $l = 15$ μm. This parameter was determined by using a microscope. The drop of urine was placed on the microscope slide with the object on the micrometer scale. The resulting film was dried at room temperature ($t = 22$°C). Later, by means of microscope overfocusing from the upper surface of the urine film to the scale of object, we measured the typical thickness of the urine polycrystalline film.

C. Experimental Measurements of the Mueller-Matrix Elements Coordinate Distributions

Measurements of the coordinate distributions of the Mueller-matrix elements were performed in the setup (Fig. 1) [10].

Illumination of samples was performed by the parallel ($\varnothing = 2 \times 10^3$ μm) weakly intensive ($W = 5$ mW) beam (1)

of a He–Ne laser ($\lambda = 0.6328$ μm). Using a collimated illuminating beam provides the same conditions of transformation of the polarization states at different points of the illuminated area of the object. In this case, our scheme provides a resolution of 4.65 μm × 4.65 μm. This scale is sufficient to evaluate the optical properties of the average (5–20 μm) crystalline structural elements of the of urine films. This allows comparative studies to differentiate different groups of samples. The polarization light source consisted of a quarter-wave plate (3) and a polarizer (4). The images of samples (6) were projected in the light-sensitive plane of a CCD camera [10; The Imaging Source DMK 41AU02.AS, monochrome 1/2" CCD, Sony ICX205AL (progressive scan), 1280 × 960 resolution, 5952 μm × 4464 μm light-sensitive plate, 0.05 lx sensitivity, 8 bit dynamic range, 9 bit SNR, and nonlinearity does not exceed 3%–5%] by means of an optical system (7). In this experimental arrangement, position 7 designates an image-forming apparatus, which consists of a strain-free objective (Nikon CFI Achromat P, 30 mm working distance, 50 mm focal distance, 0.1 NA, and 4 × magnification) and tube lens (200 mm focal distance). Polarization analysis of the samples images was performed by means of quarter-wave plate (8) and polarizer-analyzer (9).

For the series of linear (0°;45°;90°) and right- ($\otimes$) circularly polarized illuminating laser beams, the Stokes-vector parameters $S_{i=2;3;4}^{0;45;90;\otimes}$ were measured in accordance with the following algorithm:

$$\begin{cases} S_{i=1}^{0;45;90;\otimes} = U_{0}^{0;45;90;\otimes} + U_{90}^{0;45;90;\otimes}, \\ S_{i=2}^{0;45;90;\otimes} = U_{0}^{0;45;90;\otimes} - U_{90}^{0;45;90;\otimes}, \\ S_{i=3}^{0;45;90;\otimes} = U_{45}^{0;45;90;\otimes} - U_{135}^{0;45;90;\otimes}, \\ S_{i=4}^{0;45;90;\otimes} = U_{\otimes}^{0;45;90;\otimes} - U_{\oplus}^{0;45;90;\otimes}. \end{cases} \quad (6)$$

Here, $U_{0;90;45;135;\otimes;\oplus}^{0;45;90;\otimes}$ are intensities of linearly (0°;90°;45°; 135°), and right- ($\otimes$) and left- ($\oplus$) circularly polarized components of the filtered [by means of a polarizer (9) and a quarter-wave plate (8)] laser radiation.

Finally, the Mueller-matrix invariants were calculated as follows [by a PC (11)]:

$$\begin{cases} m_{44} = S_4^{\otimes} - 0.5(S_4^0 + S_4^{90}), \\ \sum m_{22;33} = m_{22} + m_{33} = 0.5(S_2^0 - S_2^{90}) + S_3^{45} - 0.5(S_3^0 + S_3^{90}), \\ \Delta m_{23;32} = m_{23} - m_{32} = S_2^{45} - 0.5(S_2^0 + S_2^{90}) - 0.5(S_3^0 - S_3^{90}), \end{cases} \quad (7)$$

using a He–Ne laser in our study conditioned by high monochromaticity, directivity, and the spectral brightness of its beam.

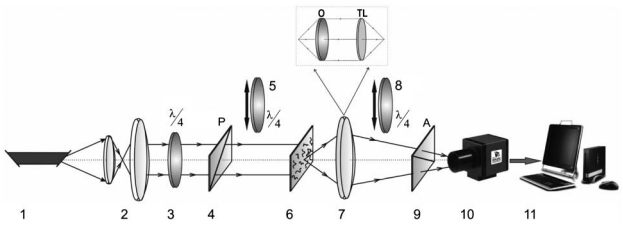

Fig. 1. Optical scheme of experimental setup. 1, He–Ne laser; 2, collimator; 3, stationary quarter-wave plate; 5,8, mechanically movable quarter-wave plates; 4,9, polarizer and analyzer, respectively; 6, object of investigation; 7, optical system; 10, CCD camera; 11, PC. Explanations are in the text.

However, the disadvantage of coherent sources is a speckle noise formation due to multiple scattering, which acts in the volume of the biological layer. To minimize this effect, we used optically thin layers. In this case, the volume of such layers implemented single scattering, which is accompanied by the formation of a polarization-inhomogeneous image without speckle background. The distributions of polarization states in this image are uniquely associated with the distribution phase anisotropy parameters, as the manifestations of dichroism or diattenuation in the "red" region of the spectrum are minimal. This allows us to solve the inverse problem—the reconstruction of the distribution of values of the phase shift between the orthogonal (linearly and circularly polarized) components of the amplitude of the laser radiation. The experimental implementation of the criterion of the single scattering mode is the value of the extinction coefficient $\tau \le 0.1$, which can be measured on the basis of Bouguer's law. For films, the urine ratio between the intensities of the incident and transmitted forward laser radiation lies in the range

$$0.9 \le \frac{I}{I_0} \le 0.93 \leftrightarrow 0.073 \le \tau \le 0.098.$$

It should be noted that polarimetric measurements can use other types of radiators or low-coherent light sources, such as LEDs or halogen bulbs equipped with a bandpath filter. On the other hand, the use of coherent laser radiation allows for integrated development and comparative analysis of the possibilities of polarimetric techniques in related areas of diagnostics, such as digital holography polarization interferometry, coherent image processing using the reference wave, and direct measurement of the Jones matrices.

D. Reconstruction of the Parameters of Optical Anisotropy

On the basis of Eq. (7) for each pixel of the CCD camera, Eq. (5) parameters of phase (δ, θ) anisotropy were found. For the objective assessment of histograms $N(q)$ of distributions $q \equiv \{\delta, \theta\}$, the set of statistical moments of the first–fourth orders was determined as

$$\begin{aligned} R_1 &= \frac{1}{P}\sum_{j=1}^{P} q_j \\ R_2 &= \sqrt{\frac{1}{P}\sum_{j=1}^{P} (q)_j^2} \\ R_3 &= \frac{1}{R_2^3}\frac{1}{P} \\ R_4 &= \frac{1}{R_2^4}\frac{1}{P}\sum_{j=1}^{P} (q)_j^4. \end{aligned} \quad (8)$$

Here, P is the number of pixels of the CCD camera. These parameters characterize the mean (R_1), dispersion (R_2), skewness (R_3), and kurtosis or "peak sharpness" (R_4) of $N(q)$.

The series of images in Figs. 2 and 3 presents the results of the technique of Mueller-matrix reconstruction parameters $q \equiv \{\delta, \theta\}$ of polycrystalline urine films. Each figure consists of the coordinate distributions [fragments (1),(3)] and the histograms $N(q)$ [fragments (2),(4)] for two arbitrary chosen samples of

healthy [fragments (1),(2)] donors and those suffering from albuminuria patients [fragments (3),(4)].

Distribution parameters of the phase anisotropy of polycrystalline films of urine were obtained on the basis of measurements within each pixel of the digital camera of the set of polarization-filtered values $I^{0;45;90;\otimes}_{0;90;45;135;\otimes;\oplus}$ of intensities of linearly (0°;90°;45°;135°), right- ($\otimes$) and left- ($\oplus$) circularly polarized components of the filtered [by means of a polarizer (9) and a quarter-wave plate (8)] laser radiation. At the next stage, the values of coordinate distributions of Stokes parameters in Eq. (6) and Mueller-matrix invariants in Eq. (7) were calculated. Obtained distributions $\{f_{44}; \sum f_{22;33}; \Delta f_{23;32}$ served as input parameters for reconstruction of the phase anisotropy parameters in Eq. (5).

Comparative analysis of the data obtained (Figs. 2 and 3) showed similar tendencies for the investigated samples:

Linear birefringence. It was determined that for the film of urine taken from a donor [Fig. 2, fragments (1)], the value of linear birefringence of lathlike globulin proteins is sufficiently less if compared to the sample [Fig. 2, fragments (3)] of albuminuria patients. The main extremes of histograms $N(\delta)$ of group 1 [Fig. 2, fragments (2)] are localized in the area of $\delta \rightarrow (0.07/0.12) \times 10^{-1}\pi$. For group 2 [Fig. 2, fragments (4)], the bigger values of phase shifts $\delta = (0.25/0.35) \times 10^{-1}\pi$ are the most probable. Thus, the increase of mean ($R_1\uparrow$) and dispersion ($R_2\uparrow$) of histograms $N(\delta)$ appears to be a statistical indicator of the albuminuria condition. Hence, the statistical moments of higher orders [skewness ($R_3\downarrow$) and kurtosis ($R_4\downarrow$)] decrease. Physically, the obtained results can be related to the known data of biochemical analysis—greater concentration of albumin in the film of urine of albuminuria patient.

Circular birefringence. Similar tendencies, related to δ, in the statistical changes of parameter θ are determined (Fig. 3), characterizing the optical activity of globulin proteins [relations (2)] in urine films. Due to the increase of concentration of such proteins in urine of albuminuria patients, the probability of greater values of θ, formed by the sample of group 2, increases [Fig. 3, fragments (3)]. Quantitatively, this illustrates the increase of probability of forming greater values $\theta = (0.4/0.75) \times 10^{-1}\pi$ in distributions $N(\theta)$ [Fig. 3, fragments (4)]. In other words, for the oncological state, the following statistical scenario is realized: $R_1(\theta)\uparrow$; $R_3(\theta)\downarrow$; $R_4(\theta)\downarrow$.

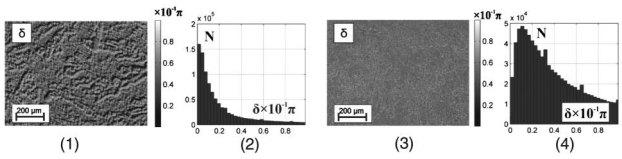

Fig. 2. (1),(3) Coordinate distributions and (2),(4) the corresponding histograms of the values of phase shifts δ, formed by polycrystalline film of (1),(2) urine of donors and (3),(4) patients with albuminuria.

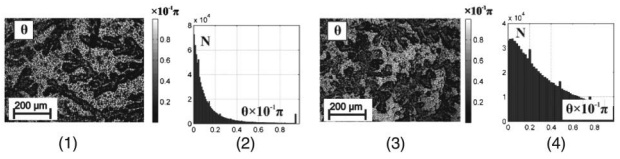

Fig. 3. (1),(3) Coordinate distributions and (2),(4) the corresponding histograms of the values of phase shifts θ, formed by polycrystalline film of (1),(2) urine of donors and (3),(4) patients with albuminuria.

E. Statistical Intergroup Analysis

For the possible clinical application of both methods, the following was determined for each group of samples [35–37]:

- average (within group 1 and group 2) values of statistical moments $R_{i=1;2;3;4}(q)$, their standard deviations $\pm\sigma$, and histograms $N(R_i)$; see Table 1.
- traditional, for probative medicine operational characteristics, sensitivity ($\mathrm{Se} = \frac{a}{a+b}100\%$), specificity ($\mathrm{Sp} = \frac{c}{c+d}100\%$), and balanced accuracy ($\mathrm{Ac} = \frac{\mathrm{Se}+\mathrm{Sp}}{2}$), where a and b are the numbers of correct and wrong diagnoses within group 2, respectively, and c and d are the same within group 1; see Table 2.

Differentiation of birefringence images of urine layers for each polarizationally reconstructed parameter of phase anisotropy was performed by cross-sectional comparison of distribution histograms $R_{i=1;2;3;4}(q)$. If the mean value of this or that moment $\bar{R}_i(q)$ in the test group 1 is not within the standard deviation σ of the investigated group 2, the difference between $\bar{R}_i(q)$ is considered statistically reliable. Then the analysis of the region of overlap of histograms $R_{i=1;2;3;4}(q)$ which determine the sensitivity Se, specificity Sp, and accuracy Ac appears to be topical.

The comparative analysis of the data obtained (Table 1) showed that the differences between the values of average $\bar{R}_{i=1;2;3;4}(q)$ moments of all orders are statistically reliable. However, there is an intergroup overlap for all histograms $N(R_i)$. Moreover, the range of such an overlap is inversely proportional to the value of the difference between the averages $\bar{R}_{i=1;2;3;4}(q)$. The following quantitative differences between average statistical moments $\bar{R}_i(q)$ are determined:

Table 2. Operational Characteristics of the Method of Mueller-Matrix Reconstruction of Polycrystalline Structure of Urine Films

q	R_i	δ (%)	θ (%)
Ac(Z_i)	R_1	74	78
	R_2	83	87
	R_3	91	90
	R_4	93	95

Table 1. Average ($\bar{R}_{i=1;2;3;4}$) and Standard Deviations ($\pm\sigma$) of Statistical Moments $R_{i=1;2;3;4}$ of Optical Anisotropy Distributions of Urine of Groups 1 and 2

	δ ($n = 57$)		θ ($n = 57$)	
q	Group 1	Group 2	Group 1	Group 2
R_1	0.09 ± 0.007	0.11 ± 0.09	0.07 ± 0.005	0.1 ± 0.007
R_2	014 ± 0.011	0.21 ± 0.016	0.11 ± 0.008	0.19 ± 0.015
R_3	0.85 ± 0.061	0.49 ± 0.036	0.96 ± 0.074	0.54 ± 0.041
R_4	1.14 ± 0.083	0.65 ± 0.047	1.34 ± 0.01	0.77 ± 0.57

Linear birefringence—for Mueller-matrix reconstructed distributions δ of polycrystalline urine films of both types, the difference between statistical moments $\tilde{R}_{i=1;2;3;4}(\delta)$ is $\{\Delta R_1(\delta) = 1.43; \Delta R_2(\delta) = 1.72; \Delta R_3(\delta) = 1.78; \Delta R_4(\delta) = 1.74\}$. Circular birefringence—for statistical moments $\tilde{R}_{i=1;2;3;4}(q)$ characterizing the distribution θ, formed by optically active structures of globulin of urine film are determined as $\{\Delta R_1(\theta) = 1.22; \Delta R_2(\theta) = 1.5; \Delta R_3(\theta) = 1.73; \Delta R_4(\theta) = 1.75\}$.

As the data presented show, the statistical moments of the third and fourth orders characterizing the histograms $N(q)$ of the urine films of both groups of patients prove to be the most sensitive. On the other hand, the greater $\Delta R_{i=1;2;3;4}(q)$ is, the more informative (Se↑; Sp↑; Ac↑) the method appears to be.

Table 2 presents the parameters of information value of the azimuthally stable method of Mueller-matrix reconstruction of phase anisotropy of polycrystalline films of urine.

The comparative analysis of operational characteristics of the method of Mueller-matrix polarization reconstruction of polycrystalline structure of urine films revealed clinically optimal (highlighted in gray) parameters

$$\begin{cases} \delta \to Z(\delta) \equiv \{\mathrm{Ac}(R_{3;4}) = 91\% - 93\%\}, \\ \theta \to Z(\theta) \equiv \{\mathrm{Ac}(R_{3;4}) = 90\% - 95\%\}. \end{cases}$$

The obtained results enable us to state a rather high level of accuracy of azimuthally stable Mueller-matrix mapping. According to the criteria of probative medicine [35], the parameters $Z(\delta, \theta) \sim 90\%$–$95\%$ correspond to high quality.

4. CONCLUSION

We have proposed a model of generalized optical anisotropy and a technique of azimuthally invariant Mueller-matrix reconstruction of optical anisotropy parameters of polycrystalline urine films. On this basis, the Mueller-matrix invariants describing the polarization nature of partial mechanisms of optical anisotropy of biological fluids were defined. By means of statistical analysis, the interconnection between the statistical moments of the first–fourth orders of anisotropy parameters of urine films and the changes in its structure in healthy people and albuminuria patients were determined. We have shown the efficiency of azimuthally invariant Mueller-matrix reconstruction of optical anisotropy parameters of urine films in the diagnostics of early stages of albuminuria.

REFERENCES

1. M. H. Smith, "Interpreting Mueller matrix images of tissues," Proc. SPIE **4257**, 82–89 (2001).
2. T. T. Tower and R. T. Tranquillo, "Alignment maps of tissues: I. Microscopic elliptical polarimetry," Biophys. J. **81**, 2954–2963 (2001).
3. J. M. Bueno and J. Jaronski, "Spatially resolved polarization properties for in vitro corneas," Ophthalmic Physiolog. Opt. **21**, 384–392 (2001).
4. M. H. Smith, P. Burke, A. Lompado, E. Tanner, and L. W. Hillman, "Mueller matrix imaging polarimetry in dermatology," Proc. SPIE **3991**, 210–216 (2000).
5. J. M. Bueno and F. Vargas-Martin, "Measurements of the corneal birefringence with a liquid-crystal imaging polariscope," Appl. Opt. **41**, 116–124 (2002).
6. T. T. Tower and R. T. Tranquillo, "Alignment maps of tissues: II. Fast harmonic analysis for imaging," Biophys. J. **81**, 2964–2971 (2001).
7. M. Shribak and R. Oldenbourg, "Techniques for fast and sensitive measurements of two-dimensional birefringence distributions," Appl. Opt. **42**, 3009–3017 (2003).
8. S. N. Savenkov, V. V. Marienko, E. A. Oberemok, and O. I. Sydoruk, "Generalized matrix equivalence theorem for polarization theory," Phys. Rev. E. **74**, 605–607 (2006).
9. Lu. R. A. Chipman, "Interpretation of Mueller matrices based on polar decomposition," J. Opt. Soc. Am. A **13**, 1106–1113 (1996).
10. O. V. Angelsky, P. V. Polyanskii, and C. V. Felde, "The emerging field of correlation optics," Opt. Photon. News **23**(4), 25–29 (2012).
11. Yu. A. Ushenko, T. M. Boychuk, V. T. Bachynsky, and O. P. Mincer, "Diagnostics of structure and physiological state of birefringent biological tissues: statistical, correlation and topological approaches," in *Handbook of Coherent-Domain Optical Methods* (Springer, 2013), p. 107.
12. O. Panchuk, A. Savitskiy, P. Fochuk, Ye. Nykonyuk, O. Parfenyuk, L. Shcherbak, M. Ilashchuk, L. Yatsunyk, and P. Feychuk, "IV group dopant compensation effect in CdTe," J. Cryst. Growth **197**, 607–611 (1999).
13. O. V. Angelsky, Yu. A. Ushenko, A. V. Dubolazov, and O. Yu. Telenha, "The interconnection between the coordinate distribution of Mueller-matrixes images characteristic values of biological liquid crystals net and the pathological changes of human tissues," Adv. Opt. Technol. **2010**, 130659 (2010).
14. V. A. Ushenko and M. P. Gorsky, "Complex degree of mutual anisotropy of linear birefringence and optical activity of biological tissues in diagnostics of prostate cancer," Opt. Spectrosc. **115**, 290–297 (2013).
15. Yu. A. Ushenko, M. P. Gorskii, A. V. Dubolazov, A. V. Motrich, V. A. Ushenko, and M. I. Sidor, "Spatial-frequency Fourier polarimetry of the complex degree of mutual anisotropy of linear and circular birefringence in the diagnostics of oncological changes in morphological structure of biological tissues," Quantum Electron. **42**, 727–732 (2012).
16. V. A. Ushenko and M. S. Gavrylyak, "Azimuthally invariant Mueller-matrix mapping of biological tissue in differential diagnosis of mechanisms protein molecules networks anisotropy," Proc. SPIE **8812**, 88120Y (2013).
17. O. V. Angel'skiĭ, A. G. Ushenko, S. B. Ermolenko, D. N. Burkovets, V. P. Pishak, Y. A. Ushenko, and O. V. Pishak, "Polarization-based visualization of multifractal structures for the diagnostics of pathological changes in biological tissues," Opt. Spectrosc. **89**, 799–804 (2000).
18. V. A. Ushenko, N. I. Zabolotna, S. V. Pavlov, D. M. Burcovets, and O. Y. Novakovska, "Mueller-matrices polarization selection of two-dimensional linear and circular birefringence images," Proc.SPIE **9066**, 90661X (2013).
19. V. A. Ushenko and A. V. Dubolazov, "Correlation and self similarity structure of polycrystalline network biological layers Mueller matrices images," Proc. SPIE **8856**, 88562D (2013).
20. K. C. Norris, N. Tareen, D. Martins, and N. D. Vaziri, "Implications of ethnicity for the treatment of hypertensive kidney disease, with an emphasis on African Americans," Nat. Clin. Pract. Nephrol. **4**, 538–549 (2003).
21. N. Boute, O. Gribouval, S. Roselli, F. Benessy, H. Lee, A. Fuchshuber, K. Dahan, M. C. Gubler, P. Niaudet, and C. Antignac, "NPHS2, encoding the glomerular protein podocin, is mutated in autosomal recessive steroid-resistant nephrotic syndrome," Nat. Genet. **24**, 349–354 (2000).
22. B. M. Brenner, *Brenner and Rector's The Kidney*, 8th ed. (Saunders, 2007).
23. Y. T. Chen, A. Kobayashi, K. M. Kwan, R. L. Johnson, and R. R. Behrionger, "Gene expression profiles in developing nephrons using Lim1 metanephric mesenchyme-specific conditional mutant mice," BMC Nephrol. **7**, 1 (2006).
24. P. N. Hawkins, "Serum amyloid P component scintigraphy for diagnosis and monitoring amyloidosis," Curr. Opin. Nephrol. Hypertens. **11**, 649–655 (2002).
25. B. G. Hudson, K. Tryggvason, M. Sundaramoorthy, and E. G. Neilson, "Alport's syndrome, Goodpasture's syndrome, and type IV collagen," N. Engl. J. Med. **348**, 2543–2556 (2003).
26. KDIGO, "Clinical practice guidelines for the evaluation and management of chronic kidney disease," Kidney Int. Suppl. **3**, 5–14 (2013).

27. L. Rampoldi, F. Scolari, A. Amoroso, G. Ghiggeri, and O. Devuyst, "The rediscovery of uromodulin (Tamm–Horsfall protein): from tubulointerstitial nephropathy to chronic kidney disease," Kidney Int. **80**, 338–347 (2011).
28. K. Tryggvason, J. Patrakka, and J. Wartiovaara, "Hereditary proteinuria syndromes and mechanisms of proteinuria," N. Engl. J. Med. **354**, 1387–1401 (2006).
29. Yu. A. Ushenko, V. A. Ushenko, A. V. Dubolazov, V. O. Balanetskaya, and N. I. Zabolotna, "Mueller-matrix diagnostics of optical properties of polycrystalline networks of human blood plasma," Opt. Spectrosc. **112**, 884–892 (2012).
30. Yu. A. Ushenko, A. V. Dubolazov, V. O. Balanetskaya, A. O. Karachevtsev, and V. A. Ushenko, "Wavelet-analysis of polarization maps of human blood plasma," Opt. Spectrosc. **113**, 332–343 (2012).
31. V. O. Ushenko, "Spatial-frequency polarization phasometry of biological polycrystalline networks," Opt. Mem. Neural Netw. **22**, 56–64 (2013).
32. V. A. Ushenko, N. D. Pavlyukovich, and L. Trifonyuk, "Spatial-frequency azimuthally stable cartography of biological polycrystalline networks," Int. J. Opt. **2013**, 1–7 (2013).
33. O. V. Angelsky, A. Ya. Bekshaev, P. P. Maksimyak, A. P. Maksimyak, S. G. Hanson, and C. Yu. Zenkova, "Self-diffraction of continuous laser radiation in a disperse medium with absorbing particles," Opt. Express **21**, 8922–8938 (2013).
34. V. P. Ungurian, O. I. Ivashchuk, and V. O. Ushenko, "Statistical analysis of polarizing maps of blood plasma laser images for the diagnostics of malignant formations," Proc. SPIE **8338**, 83381L (2011).
35. L. D. Cassidy, "Basic concepts of statistical analysis for surgical research," J. Surg. Res. **128**, 199–206 (2005).
36. C. S. Davis, *Statistical Methods of the Analysis of Repeated Measurements* (Springer-Verlag, 2002).
37. A. Petrie and B. Sabin, *Medical Statistics at a Glance* (Blackwell, 2005), 157 pages.